Magnetic Resonance Imaging Evaluation of Normal Glenoid Length and Width: An Anatomic Study

Brett A. Lenart, M.D., Ryan Freedman, B.S., Geoffrey S. Van Thiel, M.D., M.B.A.,
Aman Dhawan, M.D., Kevin C. McGill, M.D., M.P.H., Sanjib Basu, Ph.D.,
John R. Meyer, D.O., CDR Matthew T. Provencher, M.D., USNR,
Brian J. Cole, M.D., M.B.A., Anthony A. Romeo, M.D., and Nikhil N. Verma, M.D.

Purpose: The purpose of this study was to evaluate the measured dimensions of the normal glenoid on sagittal magnetic resonance (MR) imaging to determine whether a fixed ratio of glenoid length and width can be determined. **Methods:** MR images of 90 glenoids in 84 patients were analyzed. The mean age was 54.8 years, with 44 male and 40 female patients. Glenoid length and width at the widest dimension were measured and recorded by 3 independent examiners. The ratio of length to width and the ratio of the length of the superior pole at the widest point to the total length were calculated. Intraclass correlation coefficients, Spearman and Pearson correlations, regression analysis with cross validation, and coefficients of variation were calculated. **Results:** The mean glenoid length was 37.5 ± 3.8 mm, whereas the mean width was 24.4 ± 2.9 mm. The mean ratio of length to width was 1.55 ± 0.1, whereas the mean ratio of the distance from the superior pole to the widest point to the total glenoid length was 0.64 ± 0.03. The calculated ratios were less variable than the absolute length and width. Cross validation of length for width showed a 95% prediction band width of 4.48 mm, with an average absolute error of prediction of 1.46 mm, and was equally specific when separated by gender. The width was equal to 0.65 times the length. **Conclusions:** Measurement of glenoid length and width using MR imaging results in a consistent ratio of length to width independent of patient age and gender, where the width was equal to 0.65 times the length at a point two-thirds along the inferosuperior axis. **Level of Evidence:** Level IV, case series.

Arthroscopic repair for patients with recurrent instability of the shoulder remains a challenge. Failure after repair has been associated with young patient age, contact or overhead athletic activities, and most significantly, glenoid bone deficiency.[1-5] Glenoid bone deficiency is usually found in the anteroinferior region and has been observed in 8% to 73% of cases of recurrent shoulder dislocation.[1-5] Preoperative identification and quantification of glenoid bone loss are critical to determine whether patients require bone reconstruction versus soft-tissue stabilization alone.[1-6]

The use of computed tomography (CT) scan has been described for preoperative quantification of glenoid bone loss. However, magnetic resonance imaging (MRI) is often initially performed for evaluation of the soft tissues, including the capsuloligamentous structures, labrum, and rotator cuff. The additional use of CT has the potential to lead to increased costs, because it is a second diagnostic test in addition to MRI, and exposure to radiation. Thus the ability to accurately quantify glenoid bone loss on MRI would allow the use of a single study to evaluate both bone and soft-tissue pathology.

In 1992 Iannotti et al.[7] published an anatomic study of the normal glenohumeral relations. After they measured 140 cadavers, the superoinferior and lower-half anteroposterior dimensions of the glenoid were found to have some variability, although the ratio of length to width was a relative constant. By use of this information, if the length of the glenoid is preserved, even in bone loss situations, the fixed ratio could be

used to calculate the expected width of the glenoid based on the measured length. A comparison of expected width with measured width would provide an estimation of glenoid bone loss.

The purpose of this study was to evaluate the measured dimensions of the normal glenoid on sagittal MRI to determine whether a fixed ratio of glenoid length and width can be determined. Our hypothesis was that glenoid length and width can be consistently measured on sagittal MRI and that a fixed ratio based on these measurements exists.

Methods

Between 2007 and 2009, we identified 107 consecutive patients at our institution who underwent non-contrast MRI of the shoulder for evaluation of suspected shoulder pathology. We excluded 23 shoulders because of prior surgery, history or complaint of instability, appearance of anterior or posterior labral tear, or glenohumeral arthritis, leaving 90 shoulders in 84 patients for evaluation (final diagnoses included biceps tendinopathy and biceps tears, acromioclavicular degeneration, rotator cuff tendinopathy, full- and partial-thickness rotator cuff tears, degenerative labral tears, and joint effusion individually or in combination). MRI was performed using a 1.5-T Siemens Espree (Siemens, Malvern, PA) with sections of 3.5 to 4 mm, with a 1-mm gap. Oblique, coronal, and sagittal (en face) views were obtained for all patients. Three independent medical observers trained in identifying glenohumeral anatomy reviewed the images. Glenoid parameters were measured on T1-weighted sagittal oblique views. The most lateral view through the glenoid surface that allowed evaluation of the glenoid perimeter without interference from the humeral head was used.

The superoinferior dimension, or length (L), was measured by drawing a straight line from the base of the coracoid process to the inferior glenoid rim, along the long axis of the glenoid. The width (W) was defined as the largest anteroposterior measurement in the lower two-thirds of the glenoid. This distance has been shown to represent the diameter of the circle formed by the inferior glenoid.[8-10] Measurements were taken at the approximation of the bony rim of the glenoid and the chondrolabral junction on the selected image. The point of intersection of the width along the length of the glenoid was recorded as the distance above the level of the width to the superior pole (A) and the distance below the level of the width to the inferior pole (B) such that A + B = L (Fig 1). The ratio of this point, A/L, was also calculated and recorded.

Statistical Analysis

Descriptive statistics (mean, median, standard deviation, and range) for measurements L, W, A, and B, as
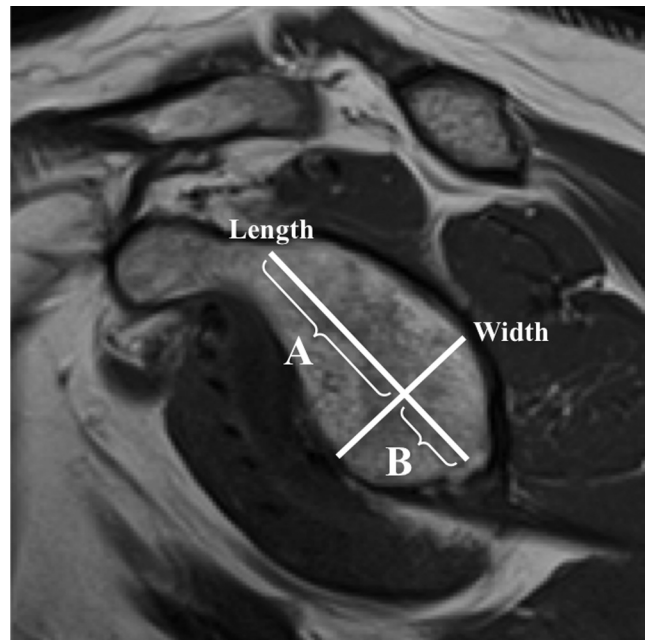

Fig 1. Sagittal oblique MR image of a normal shoulder. Length (L) was measured from the most superior point of the glenoid to the inferior rim along its axis. Distance A represents the length of the segment from the superior pole to the widest point, whereas distance B is the length of the segment from the widest point to the inferior pole, such that A + B = L.

well as the ratios L/W, A/B, and A/L, were obtained. For each variable (L, W, A, and B), an intraclass correlation coefficient (ICC) was calculated to quantify agreement between measurements. ICC values of 0.3 to 0.4 were considered fair correlations; 0.5 to 0.6, moderate; 0.7 to 0.8, strong; and greater than 0.8, near perfect. The association with age was also measured by Pearson and nonparametric Spearman correlations. The differences between the genders were assessed by 2-sample t test, as well as its nonparametric equivalent, the Mann-Whitney test. All reported P values are 2 sided, and P values between .05 and .10, between .01 and .05, and less than .01 are considered marginally significant, significant, and strongly significant, respectively.

Linear regression analysis was used to fit a model for consistent width-to-length ratio subject to sampling variability. This model implies a straight line through the origin (no intercept) on width versus length, which was fitted by regression methods. This model was further validated by repeated cross validations in which the data were randomly split into a sample set and a validation set in a 2:1 ratio. The regression model implying consistent width-to-length ratio was fit on the sample set, and the fitted models were then used to predict the width (the outcome variable) on the validation set from the length measurements. The process of randomly splitting the data in a 2:1 ratio of sample and validation sets was then repeated 5,000 times, and 95% cross-validated prediction intervals were

Table 1. Normal Glenoid Parameters Measured by MRI

	No. of Glenoids	Mean	SD	Range	Median
L	90	37.5 mm	3.8 mm	29.4-44.8 mm	37.1 mm
W	90	24.4 mm	2.9 mm	17.9-30.1 mm	24.0 mm
L/W	90	1.55	0.10	1.39-1.88	1.53
A	90	23.9 mm	2.5 mm	18.7-30.4 mm	23.7 mm
B	90	13.6 mm	1.8 mm	9.5-18.7 mm	13.3 mm
A/B	90	1.81	0.23	1.27-2.52	1.79
A/L	90	0.64	0.03	0.56-0.71	0.64

constructed based on these repeated predictions. The cross validation is a way of estimating how accurately this predictive model will perform in a clinical setting using new patients.

Statistical analyses were performed with PASW statistical software, version 18 (formerly known as SPSS; IBM, Armonk, NY), and R statistical software (Free Software Foundation, www.r-project.org). This study was approved by the institutional review board.

Results

The mean age of the patients was 54.8 years, with a range of 17 to 79 years. There were 44 male and 40 female patients. The mean length (L) ($\pm$ standard deviation) was 37.5 $\pm$ 3.8 mm, whereas the mean width (W) was 24.4 $\pm$ 2.9 mm. The distance from the superior pole to the intersection point between the length and width (A) measured 23.9 $\pm$ 2.5 mm, whereas the distance from that same point to the inferior pole (B) was 13.6 $\pm$ 1.8 mm (Table 1).

The mean L/W ratio was 1.55 $\pm$ 0.10. The mean A/B ratio was 1.81 $\pm$ 0.23 whereas the mean A/L ratio was 0.64 $\pm$ 0.03, showing that the widest point of the glenoid was consistently located at the bottom one-third of its long axis (Table 1).

ICCs were calculated for L, W, A, and B. We found that L and W showed strong correlations whereas A and B showed positive correlations (Table 2). Pearson and Spearman correlation with age was not significant for any of the observers with any individual parameter or ratio (data not included). There were strongly significant differences between male and female patients in L, W, A, and B ($P < .001$ from both 2-sample t tests and nonparametric Mann-Whitney tests) (Table 3). However, the difference in the L/W ratio was only marginally significant between the 2 genders ($P = .07$), whereas the differences in the A/B and A/L ratios were not found to be significant ($P = .81$ and $P = .92$, respectively).

Table 2. ICCs for Each Measurement

Variable	ICC	95% Confidence Interval
L	0.812	0.747-0.865
W	0.766	0.688-0.830
A	0.601	0.490-0.700
B	0.454	0.327-0.575

Table 3. Comparison of Glenoid Parameters by MRI Between Genders

	Mean		*P* Value	
	Male	Female	*t* Test	Mann-Whitney
L	40.0 mm	34.8 mm	<.001	<.001
W	26.2 mm	22.3 mm	<.001	<.001
L/W	1.53	1.57	.07	.08
A	25.5 mm	22.2 mm	<.001	<.001
B	14.5 mm	12.6 mm	<.001	<.001
A/B	1.82	1.80	.81	.59
A/L	0.64	0.64	.92	.57

NOTE. Statistical significance was determined by a 2-sample t test; equal variances were not assumed. There were 40 female patients and 44 male patients.

Linear regression analysis was used to fit a regression line with no intercept on W versus L (Fig 2). The fitted line modeled W to be equal to 0.65 times L (W = 0.65 $\times$ L). Figure 2 also shows the observed values (L and W) for measurements that clustered near the fitted regression line. The 95% confidence interval for our regression model coefficient, 0.65, was 0.6430 to 0.6645. The fit of the regression model was further examined by repeated cross validations in which the data were randomly split into a sample set and a validation set in a 2:1 ratio—that is, n = 60 and n = 30 in the sample set and validation set, respectively. The regression model was then fit on the sample set, and the fitted model was used to predict W on the validation set from L. The process of randomly splitting the data in a 2:1 ratio of sample and validation sets, fitting the regression model, and predicting W for the validation set was repeated 5,000 times, each time resulting in a possibly slightly different fitted regression model. Figure 3 shows the predicted W values from 5 randomly selected repetitions, as well as the 95% cross-validated prediction band constructed based on all 5,000 repeated predictions. The mean width of the 95% cross-validation prediction band was 4.48 mm, with a
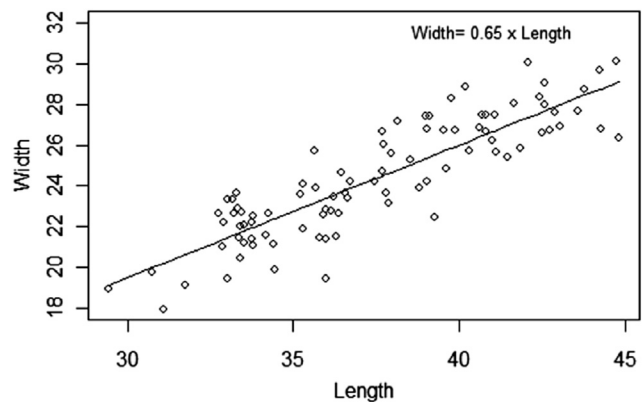

Fig 2. Plot of W versus L with regression line. Data were plotted, and a regression line without intercept was fitted. The calculated regression line was W = 0.65 $\times$ L. Data are presented in millimeters.
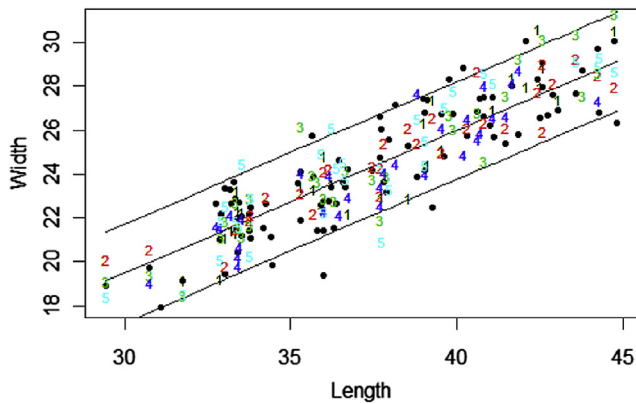
Fig 3. Cross-validation model. The central line is the linear regression line, W = 0.65 × L. The outer lines represent the 95% prediction band limits for 5,000 runs of randomly selected cases: 60 training cases and 30 validation cases. The solid data points represent the actual measurement pairs of L and W from the study. Data are presented in millimeters.

half width of 2.24 mm. The mean absolute error of prediction (absolute difference between prediction and actual value) was 1.46 mm.

Similar linear regression and cross validation were performed for the male and female subgroups. For the female subgroup, similar relations between W and L were found: the linear regression line–modeled W was equal to 0.64 times the L (W = 0.64 × L) (Fig 4). The mean width of the 95% cross-validation prediction band was 4.53 mm, with a half width of 2.27 mm. The mean absolute error of prediction was 1.47 mm. For the male subgroup, the linear regression line–modeled W was equal to 0.65 times the L (W = 0.65 × L) (Fig 5). The mean width of the 95% cross-validation prediction band was 4.50 mm, with a half width of 2.25 mm. The mean absolute error of prediction was 1.48 mm. The W could accurately predict the L when the population was analyzed as a whole, in addition to separation by gender. Similar results were found when a linear regression and cross-validation model were used to predict L based on W (data not shown).

To better compare the variability between measurements L, W, A, and B (which are measured in millimeters) with the unit-less ratios L/W, A/B, and A/L, we calculated coefficients of variation (CVs) (calculated as the ratio of standard deviation to mean) (Table 4). The CV of L/W was 0.117, less than both L and W individually. The CV of A/L, 0.109, was also less than A and B individually. When separated into male and female subgroups, the CVs were smaller for each of the individual parameters L, W, A, and B as compared with the total population, suggesting more uniformity of these parameters within gender. In addition, the CVs for the ratios of L/W and A/L for each gender were also smaller in comparison with the population analyzed as a whole.
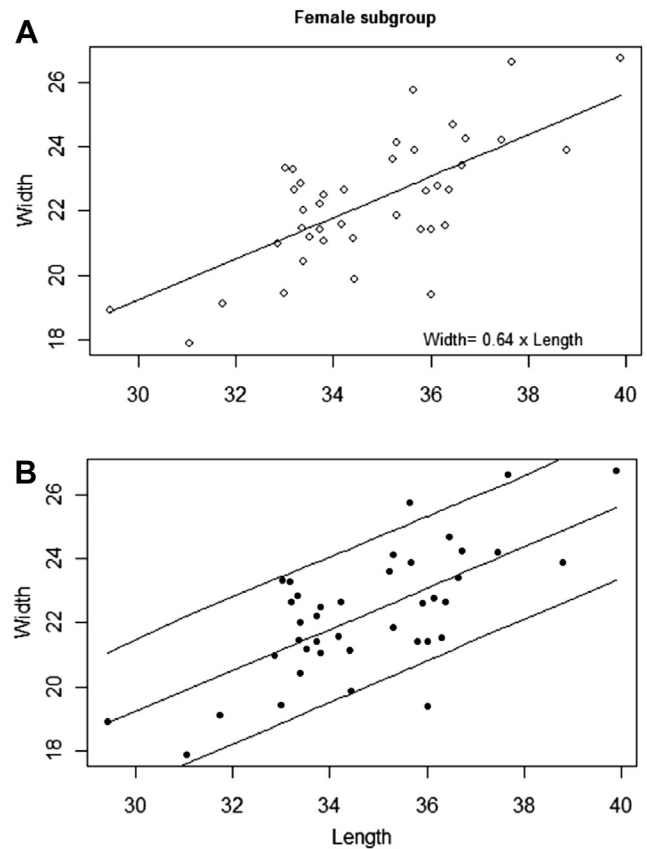

Fig 4. (A) Plot of W versus L with regression line for the female subgroup. (B) Cross-validation model for female subgroup. The central line is the linear regression line, W = 0.64 × L. The outer lines represent the 95% prediction band limits for 5,000 runs of randomly selected cases: 60 training cases and 30 validation cases. The solid data points represent the actual measurement pairs of L and W from the study. Data are presented in millimeters.

Discussion

Detection and treatment of glenoid bone deficiency remain significant obstacles in the treatment of recurrent shoulder instability. Recent technologic advances in radiographic imaging and arthroscopic techniques have prompted researchers to focus their efforts on improving detection and quantification of glenoid bone loss in the preoperative setting. The purpose of this study was to evaluate the relation between glenoid length and width, measured on a single sagittal magnetic resonance (MR) image, in normal subjects, without a history of shoulder instability. Our results indicate that this ratio, though not fixed, is relatively consistent and may prove useful in the future for quantification of glenoid bone loss in patients with instability.

CT has been classically used to characterize glenoid bone loss in patients with glenohumeral instability. Though effective in identifying osseous changes, CT is not optimal in characterizing soft-tissue pathology. Furthermore, CT carries a significant risk of exposure to ionizing radiation. In contrast, MRI allows for characterization of
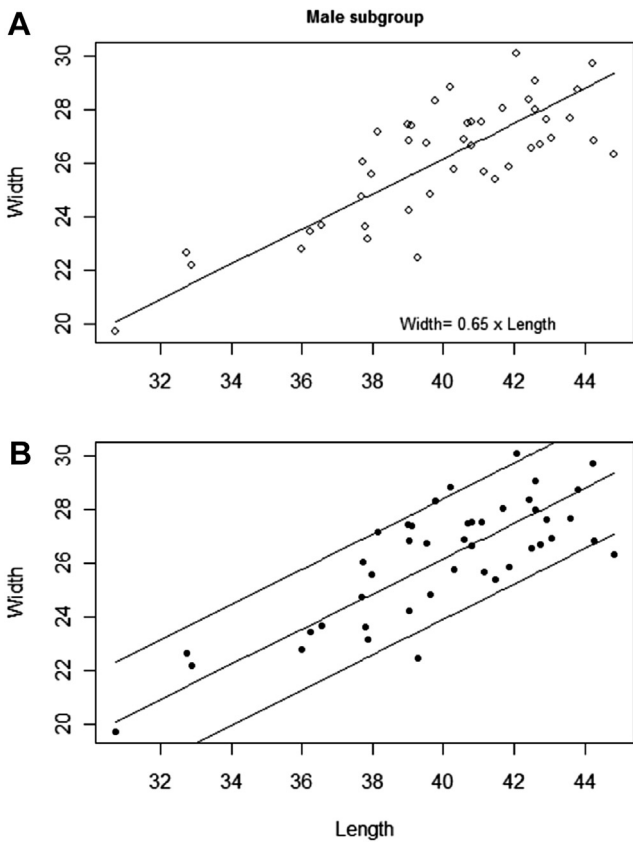
Fig 5. (A) Plot of W versus L with regression line for the male subgroup. (B) Cross-validation model for male subgroup. The central line is the linear regression line, W = 0.65 × L. The outer lines represent the 95% prediction band limits for 5,000 runs of randomly selected cases: 60 training cases and 30 validation cases. Data points plotted and numbered 1 through 5 represent the first 5 runs. The solid data points represent the actual measurement pairs of L and W from the study. Data are presented in millimeters.

the soft tissue but has traditionally been limited in the ability to accurately quantify bone loss when present.

In this study we identified normal glenoid parameters by MRI. Reproducibility of measurements was verified by calculation of the ICCs between measurements. Glenoid length was found to be slightly greater than 1.5 times glenoid width, and glenoid width and length were found to consistently intersect in the inferior one-third of the glenoid. As expected, measurements of L, W, A, and B were significantly different between male and female patients. However, ratios L/W, A/B, and A/L were found to be consistent and were not significantly different. Although the CVs for these ratios were smaller for male patients or female patients separately versus the

Table 4. CVs of Measured Glenoid Parameters by MRI

	L	W	L/W	A	B	A/B	A/L
All	0.139	0.152	0.117	0.142	0.169	0.161	0.109
Male	0.078	0.086	0.056	0.080	0.126	0.125	0.046
Female	0.059	0.089	0.067	0.064	0.103	0.130	0.042

total population, our cross-validation model confirmed accurate prediction of W based on L (W = 0.65 × L) regardless of gender. This suggests a consistent relation of these variables across gender. As expected, there was no correlation of any glenoid parameters with age. Although the CVs for all measurements were relatively low, the value was found to be greater for individual variables than ratios L/W and A/L, suggesting that these ratios are more consistent, with less variation across this patient population. The accuracy of the cross-validation model confirms the predictive ability of this model when applied to new patients.

Our results may propose a simple model for calculation of bone loss based on MRI. For any measured length, a normal, or expected, width can be calculated. This width can be compared with MR image measurement of bone width, and an estimation of bone loss can be calculated. For example, a glenoid length of 37 mm would suggest a respective width of 24.05 mm. If MR image measurement of the residual width yielded a value of 20 mm, measured two-thirds from the superior point of the glenoid, then estimated bone loss by the glenoid rim distance formula would be 16.6%.[6,11,12] Our formula for estimation of normal glenoid width is based on measurement of glenoid length from MRI. This model assumes a more anterior orientation of bone loss. Because bone loss can occur in different planes and orientations,[13,14] further studies will be needed to validate the use of our model in other models of bone loss.

Our results are consistent with data presented by Iannotti et al.[7] in an anatomic study examining normal glenohumeral parameters. In their study, 140 shoulders were evaluated: 96 nonarthritic cadaveric specimens and 44 shoulders in living subjects with 1.5-T MRI with a 3-mm slice thickness. The mean superoinferior and lower-half anteroposterior dimensions for all glenoids, both cadaveric and those assessed by MRI, were 39 ± 3.5 mm and 29 ± 3.2 mm, respectively. Similarly, our results for measurements made by MRI were 37.5 ± 3.8 mm for length and 24.4 ± 2.9 mm for width. The ratio of the length to the greatest measured width in the study by Iannotti et al. was 1.42 ± 0.20, whereas ours was 1.55 ± 0.10. This may be explained by a different distribution of data in the sample population used in each study, differences in the thickness of MR sections (3.5 to 4 mm *v* 3 mm), and the use of cadaveric specimens for measurements in the study by Iannotti et al. No evaluation of the point of greatest width along the length axis was made in the prior study. There are several key features that differentiate our study from their study. We examined correlations between glenoid parameters and ratios with both gender and age. Furthermore, our study presents data measured entirely from MRI in live patients. Both cadaveric and live patients assessed by MRI were used in the study by Iannotti et al., although no significant differences between the 2

were found. We also measured the A/L ratio, representing the location of the point of greatest glenoid width along the glenoid length. We found the widest point of the glenoid to be consistently located at the inferior one-third of the glenoid length. Lastly, we characterized variation in measurements of both parameters and calculated ratios. Although glenoid parameters may be more accurately measured by use of cadaveric specimens, in practice MRI may be the only available data source in the estimation of preoperative bone loss. However, the differences between the calculated ratios of length to width may preclude the clinical usefulness of either ratio.

Regression analysis formulas were applied to the glenoid parameter dataset to predict the width measurements for each glenoid. The regression model was validated using a 2:1 split of the data. The cross-validation model identified a 95% prediction band width of 4.48 mm, with a half width of 2.24 mm. Our model showed accurate results with a standard deviation similar to that found in published data from cadaveric specimens.[7]

Limitations

There are many sources of error to be considered. The population of patients who underwent MRI of the shoulder initially presented to the clinic with shoulder pain. Thus they do not represent a random sample from a given population, and some degree of selection bias may be present. Second, there is some variation in MR images between slice location and the actual glenoid face. Because the data are not reconstituted as is performed in 3-dimensional CT reconstruction, the use of MRI requires that the reviewer choose the best image to approximate a sagittal view of the glenoid face. In addition, the point of measurement in our study was an estimation of the edge of the bony glenoid. Our inability to accurately determine the bone-labral junction may account for some variability, which can be influenced by the thickness of the section, location of the section, angle of sectioning, and presence or absence of a labral tear or fraying. Next, our study has only evaluated the consistency of the ratio in normal patients. Further adaptation and validation of the technique in clinical bone loss models need to be completed. This model may be most accurate for estimation of anterior bone loss and may underestimate other types of bone loss, including that located more inferiorly. Although our model shows a consistent relation between glenoid length and width, it does imply that the length is a fixed variable whereas the width is a random variable. Our model does not incorporate the possibility that both length and width may be random variables. Thus its application may be limited, and a more complex model may be necessary. Finally, measurements made by MRI are limited by the strength of the scanner, slice thickness, and resolution of the images.

Conclusions

Measurement of glenoid length and width using MRI results in a consistent ratio of length to width independent of patient age and gender, where the width was equal to 0.65 times the length at a point two-thirds along the inferosuperior axis.

References

1. Fujii Y, Yoneda M, Wakitani S, Hayashida K. Histologic analysis of bony Bankart lesions in recurrent anterior instability of the shoulder. *J Shoulder Elbow Surg* 2006;15: 218-223.
2. Tauber M, Resch H, Forstner R, Raffl M, Schauer J. Reasons for failure after surgical repair of anterior shoulder instability. *J Shoulder Elbow Surg* 2004;13: 279-285.
3. Boileau P, Villalba M, Hery JY, Balg F, Ahrens P, Neyton L. Risk factors for recurrence of shoulder instability after arthroscopic Bankart repair. *J Bone Joint Surg Am* 2006;88: 1755-1763.
4. Burkhart SS, Danaceau SM. Articular arc length mismatch as a cause of failed Bankart repair. *Arthroscopy* 2000;16: 740-744.
5. Burkhart SS, De Beer JF. Traumatic glenohumeral bone defects and their relationship to failure of arthroscopic Bankart repairs: Significance of the inverted-pear glenoid and the humeral engaging Hill-Sachs lesion. *Arthroscopy* 2000;16:677-694.
6. Provencher MT, Bhatia S, Ghodadra NS, et al. Recurrent shoulder instability: Current concepts for evaluation and management of glenoid bone loss. *J Bone Joint Surg Am* 2010;92(suppl 2):133-151.
7. Iannotti JP, Gabriel JP, Schneck SL, Evans BG, Misra S. The normal glenohumeral relationships. An anatomical study of one hundred and forty shoulders. *J Bone Joint Surg Am* 1992;74:491-500.
8. De Wilde LF, Berghs BM, Audenaert E, Sys G, Van Maele GO, Barbaix E. About the variability of the shape of the glenoid cavity. *Surg Radiol Anat* 2004;26:54-59.
9. Huysmans PE, Haen PS, Kidd M, Dhert WJ, Willems JW. The shape of the inferior part of the glenoid: A cadaveric study. *J Shoulder Elbow Surg* 2006;15: 759-763.
10. Sugaya H, Moriishi J, Dohi M, Kon Y, Tsuchiya A. Glenoid rim morphology in recurrent anterior glenohumeral instability. *J Bone Joint Surg Am* 2003;85:878-884.
11. Burkhart SS, Debeer JF, Tehrany AM, Parten PM. Quantifying glenoid bone loss arthroscopically in shoulder instability. *Arthroscopy* 2002;18:488-491.
12. Itoi E, Lee SB, Amrami KK, Wenger DE, An KN. Quantitative assessment of classic anteroinferior bony Bankart lesions by radiography and computed tomography. *Am J Sports Med* 2003;31:112-118.
13. Saito H, Itoi E, Sugaya H, Minagawa H, Yamamoto N, Tuoheti Y. Location of the glenoid defect in shoulders with recurrent anterior dislocation. *Am J Sports Med* 2005;33:889-893.
14. Dumont GD, Russell RD, Browne MG, Robertson WJ. Area-based determination of bone loss using the glenoid arc angle. *Arthroscopy* 2012;28:1030-1035.